Nucleosynthesis Calculations with Varying β-decay Rates

Student: Molly Kaufold[1]
Mentors: Kelsey Lund[1], Sanjay Reddy[1]
[1]Institute for Nuclear Theory, University of Washington, Seattle, WA, 98105, USA

September 10, 2025

Abstract

The rapid neutron capture process (r-process) is a complex and interesting nuclear physics phenomenon that is responsible for synthesis of actinides and about half the material heavier than iron in the universe. The astrophysical site of the r-process remains widely debated, but a promising and largely supported location is in the outflows of neutron star mergers. Within the r-process, there are many nuclear uncertainties that can make nucleosynthesis calculations difficult, and therefore on a much larger scale, make predictions of a merger's observables challenging to quantify. One of these uncertainties is beta decay rates. Beta decays are in active competition with both the neutron capture rates early on in the r-process and with other decay modes for heavier nuclei later in the r-process. These rates have an effect on the distribution of material on the N-Z plane and can greatly alter the prediction of post-merger isotopic compositions. In this project, we perform nucleosynthesis calculations for a set of tracers that describe a 3D simulated post-merger accretion disk while varying theoretical beta decay rates for nuclei far from stability. We find that varying the beta decay rates has an impact on the abundances produced 1 GYr post-merger, including the actinides, which could have an impact on predictions of the ages of r-process enhanced, metal-poor stars.

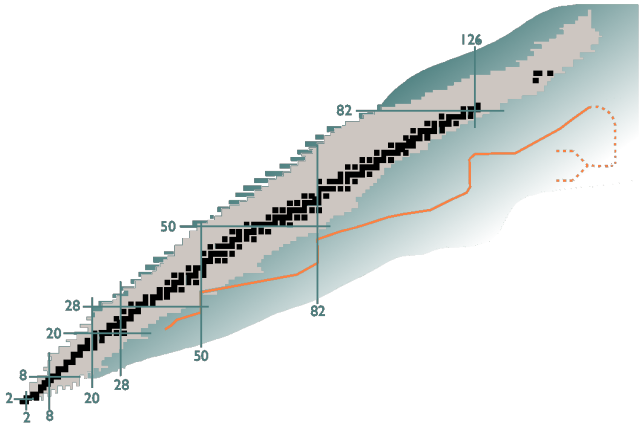

Figure 1: Chart of the nuclides with increasing proton number upwards and neutron number to the right. Stable nuclei are shown as black squares. *Figure adapted from [1].*

1 Introduction

1.1 The r-Process and Beta Decay

The rapid neutron capture process (r-process), responsible for the formation of about half the material heavier than iron in the universe and the only known natural mechanism for actinide production, occurs far from stability and in intense astrophysical environments. While the astrophysical location of this process is still debated, neutron star mergers have been linked to the r-process due to their potential to create outflow conditions of high free neutron density [2]. Neutron stars are dense, neutron rich stars that are the remnants of core collapse supernovae [3]. In the event of the collision of two neutron stars, the inspiral and merger can unbind large amounts of neutron-rich material, either dynamically or from an accretion disk formed after the merger. The high number of free neutrons in this ejecta, characterized by low electron fraction (Y_e) values of < 0.25, make neutron star mergers a promising site for the r-process. This hypothesis gained observational support thanks to the gravitational-wave event, GW170817 [4, 5]. The accompanying multi-wavelength electromagnetic observations following the merger indicated a slowly declining, long-wavelength signal consistent with the presence of high-opacity lanthanides synthesized in the merger ejecta [6, 7, 8].

The high abundance of free neutrons allows the neutron capture process to proceed very rapidly, moving material very far from stability, and potentially all the way out to the neutron drip line. Far from stability, and at high mass number, beta decay rates play a huge role in determining the time-scale and final outcomes of the r-process [9]. Early in the r-process beta decay rates most directly compete with neutron capture rates, dictating how far from stability material can get, and what the pattern that decays towards stability looks like. Later on in the r-process, especially for heavy nuclei, there are additional sources of competition, those from other decay rates such as alpha decay and spontaneous fission. A typical r-process path can be seen in Figure 1, represented by the orange line. This process is populated by all the timescales in competition, and might be altered with different beta decay rates. To test this, we conducted nucleosynthesis calculations using two different theoretical beta decay rates to probe all sources of competition and see how their resulting final abundance patterns differ from one another.

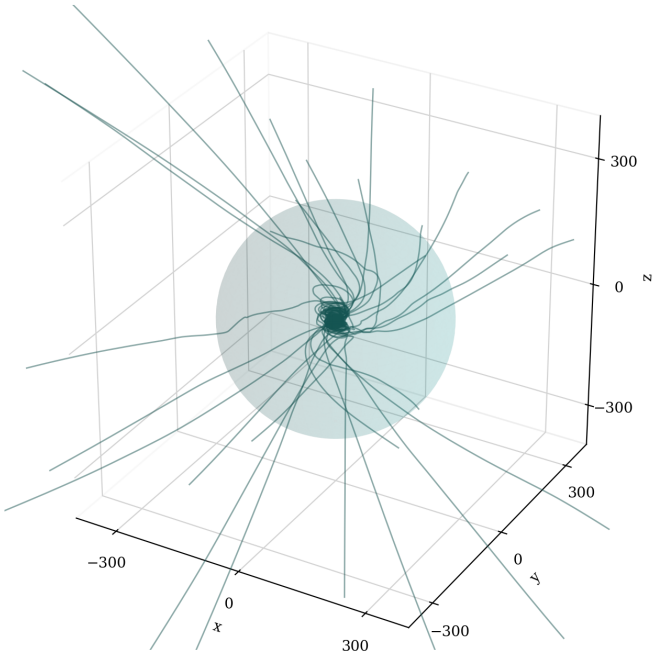

Figure 2: Visulization of tracer particles in simulation.

1.2 3D Black Hole Accretion Disk Simulation

One key ingredient for nucleosynthesis calculations is a description of the evolution of the thermodynamic conditions in the fluid where the nuclear processes take place. This project uses tracers from a 3D general-relativistic magnetohydrodynamics (GRMHD) simulation of a black hole accretion disk system with a strong magnetic field ($\beta = 10$) in order to make nucleosynthesis calculations. This simulation was carried out with nubhlight [10], a 3DGRMHD code; the details of the simulation used in this work are included in [11].

The thermodynamic evolution of the fluid in this simulation is tracked using lagrangian tracers. In this case, a lagrangian tracer refers to the tracking of fluid elements over time [12]. At the beginning of the simulation, $1.5 * 10^6$ tracer particles are uniformly sampled where there is physical fluid. These particles are then tracked over time as they undergo thermodynamic evolution.

For this project, 30 tracers were selected from more than $195,000$ unbound tracers from the simulation in order to make a more manageable dataset. These tracers were picked based on bins of electron fraction (Y_e) and radial velocity to sample the conditions described by the full set of tracers. Each tracer has an assigned identifier and mass, which is given based on the mass in each Y_e and radial velocity bin. A visualization of the spatial evolution of the tracers is given in Figure 2. The dataset for these tracers was downloaded from [13].

2 Nucleosynthesis Calculations

2.1 PRISM

For the 30 tracers described in the previous section, we perform two sets of individual nucleosynthesis calculations. In each case, we use PRISM (Portable Routines for Integrated Nucleosynthesis Modeling) version 1.6.0 developed by T. Sprouse and M. Mumpower [14]. PRISM is a modern

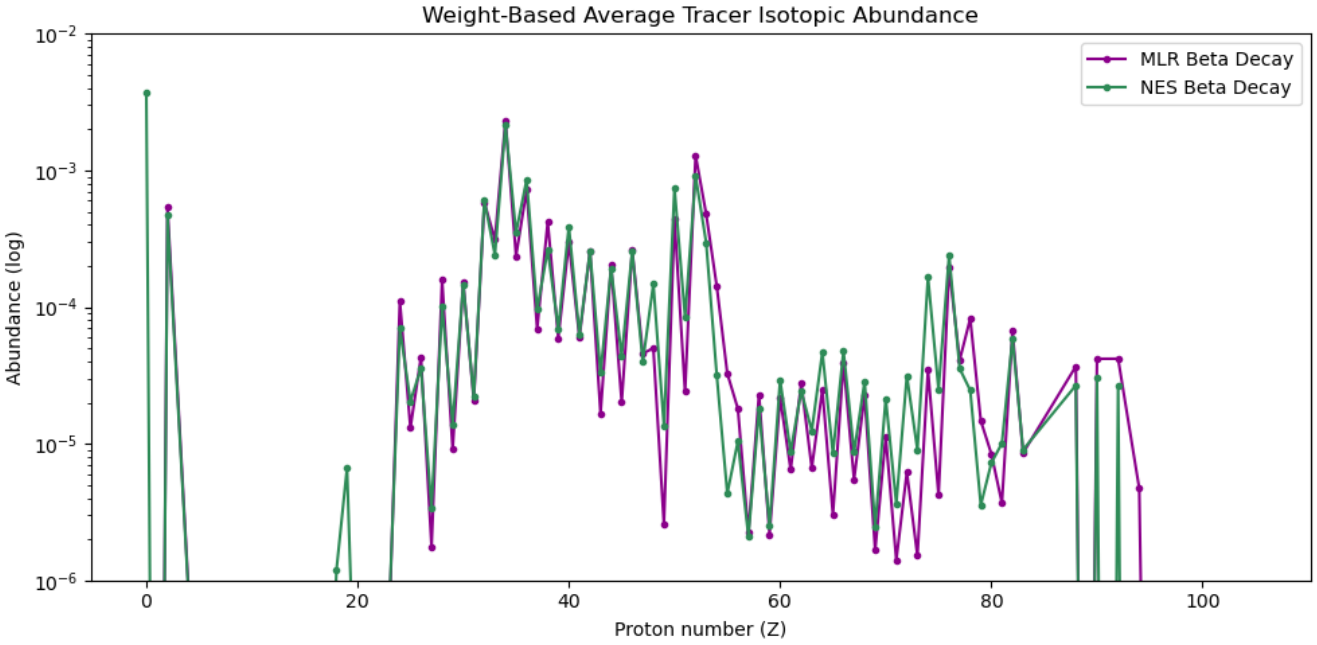

Figure 3: Abundance plot of NES and MLR beta decay rate nucleosynthesis calculations.

object-oriented Fortran nuclear network code made to track the evolution of nuclear compositions over time. The program runs based on a control file that takes nuclear data sets in a hierarchical order, as well as the specifications of the evolving astrophysical conditions. The two sets of control files created for each tracer differ by the description of beta decay (as well as accompanying beta-delayed fission) rates. We use the global beta decay rates as described in [15] (MLR) for one set of calculations, and those described in [16] (NES) for the other set. On-average, NES decay rates predict slower rates above the N=126 shell closure, where MLR decay rates are slightly faster.

A total of 60 individual nucleosynthesis calculations were carried out through the program, resulting in abundance yields sorted by proton number for each tracer. All calculations began at 1 GK and ran up to 1 GYr post neutron star merger.

2.2 Results

To compare the effect of the two sets of decay rates on the final elemental composition, we made a composite graph of all 30 tracers using a weight-based sum of each individual tracer using Python, shown in Figure 3. Each of the tracer's assigned masses were made into a percentile out of 1, to then multiply the relative abundances by and sum to obtain a singular line for plotting. As seen in the figure, both the NES and MLR decay rates tend to output fairly similar amounts of r-process products. However, it is important to note that the NES decay rates produced slightly less uranium and thorium than the MLR decay rates.

2.3 Discussion of Results and Uncertainty

The higher abundance of actinides in Figure 3 by MLR decay rates may be attributed to nuclear branching ratios and their influence on decay rate competition. With heavy nuclei, beta decay is in constant competition with other decay processes, such as fission. Varying the beta decay rates can therefore alter the outcome of this competition. With the slower NES decay rates, it may be

more likely that the nuclei will undergo fission. This is not conducive towards the building up of actinides as fission drives material away from actinides and towards lower proton and neutron numbers. With MLR's slightly faster beta decay rate, more actinides are synthesized. Fission rates are included in our nucleosynthesis calculations, so the competition between different decay rates is a large factor in differing abundance patterns. However, there is some uncertainty coming from the competing decay rates, such as other fission and alpha decay rates for example, that are not entirely known and not varied in this particular experiment. Similarly, fission yield and fission barrier heights are an additional source of uncertainty and not varied in this project.

The resulting abundances depend on theoretical nuclear physics models for unstable nuclei that exist far from stability, and which are still widely disputed. Our nucleosynthesis results are given as a model of comparison rather than a complete and definite picture of the elemental production capabilities of this particular astrophysical environment. In this project, we look at the post-merger accretion disk, but there is also a dynamical component to the ejecta that is not taken into consideration. This component consists of material that is unbound from the binary system on very short time scales. Material that is tidally disrupted directly from the neutron star is thought to be characterized by very low Y_e values, while shock- and contact-driven outflows are thought to be of higher Y_e. Together, these could potentially be a source of additional r-process production. Without considering the dynamical component of the merger, we are missing part of the whole picture of this astrophysical system.

This project serves as the starting point of a more comprehensive dive into the nuclear physics occurring in such complex environments. Looking into the future, we would like to include these sources of uncertainty in order to have a more well-rounded picture of what is occurring in this environment.

3 Future Studies

There are many different directions into which this research can continue. The two most prevalent ones include adding sources of previously stated uncertainty into consideration, as well as efforts in nuclear cosmochronometry.

3.1 Metal-Poor Stellar Compilation and Nuclear Cosmochronometry

The technique of nuclear cosmochronometry can be studied using our abundances from nucleosynthesis calculations in comparison with those from previous literature. The results of the r-process can enrich surrounding material, and become the initial abundance of a star [17]. Specifically, there exists a population of metal-poor stars (as defined by their abundance of iron compared to the solar abundance [18]) that are rich in r-process elements. The existence of these stars offers the opportunity to directly probe r-process abundance patterns synthesized by one or a few r-process-producing events. By comparing the initial abundances of a particular nuclear species with a known half-life via the nucleosynthesis-calculated abundances as well as their abundances after an unknown amount of time (the observed stellar abundances) the following equation (equation 14 in [9]) can be used to determine t, the time passed from the synthesis of species to its observation:

$$t = 21.80[log_\epsilon(U/Th)_i - log_\epsilon(U/Th)_{obs}] \quad (1)$$

We are specifically using thorium and uranium as they are actinides with distinctly long half-lives. It is important to note that uranium specifically is difficult to measure, so the amount of metal-poor stars with uranium abundances may be limited compared to that of thorium. An in-progress

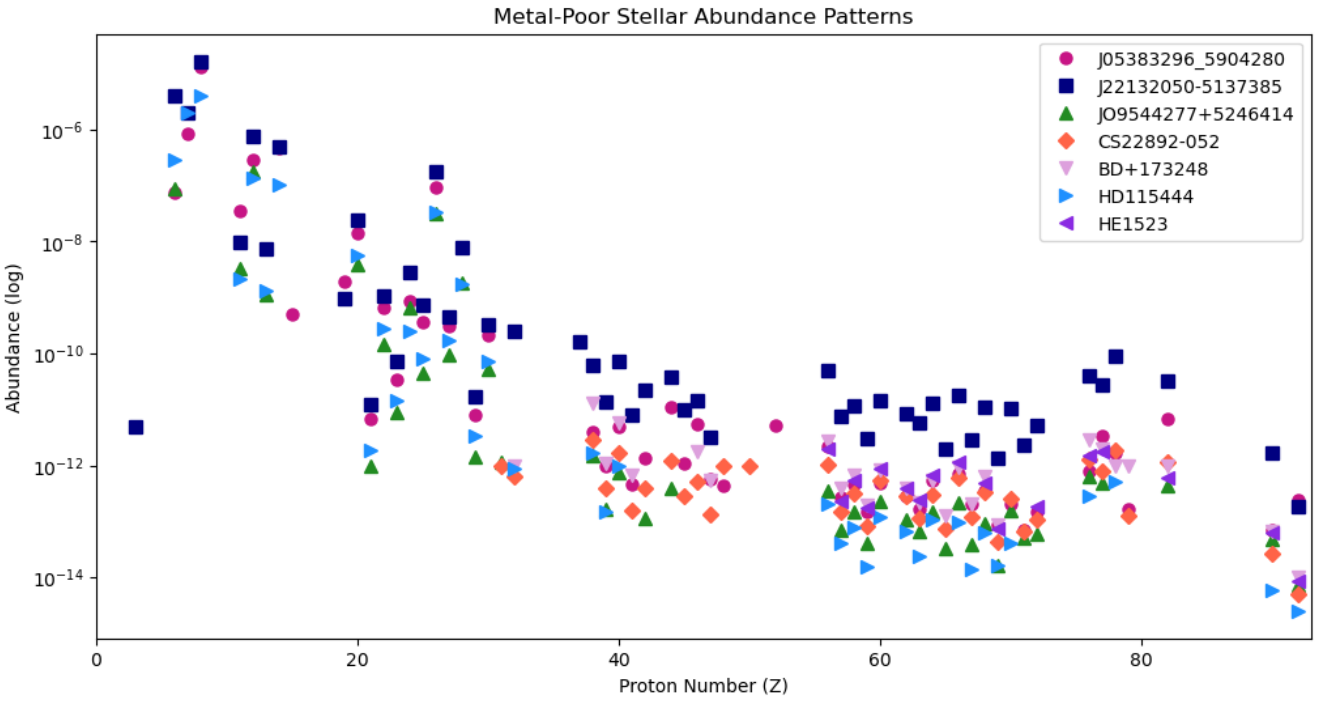

Figure 4: A compiled abundance graph of seven metal-poor stars.

catalog of r-process enhanced metal-poor stars and their relative abundances can be seen in Figure 4. Continuing the search for metal-poor stars will unlock more potential for stellar aging as well as insights into the r-process observables across the universe.

Acknowledgment

This research was supported by the INT's U.S. Department of Energy grant No. DE-FG02-00ER41132, as well as N3AS's National Science Foundation award No. 2020275. All nucleosynthesis calculations in this work were completed on Hyak, UW's high performance computing cluster. This resource was funded by the UW student technology fee.

References

[1] F. Timmes. *Nuclide Charts from cococubed*. URL: `https://cococubed.com/pix_pages/nuclide_chart.shtml`.

[2] E. Symbalisty and D. N. Schramm. "Neutron Star Collisions and the r-Process". In: *ApJ Letters* 22 (Jan. 1982), p. 143.

[3] Sunny Ng et al. "Inferring the neutron star equation of state with nuclear-physics informed semiparametric models". 2025. arXiv: `2507.03232`.

[4] B.P. Abbott, LIGO Scientific Collaboration, and Virgo Collaboration. "GW170817: Observation of Gravitational Waves from a Binary Neutron Star Inspiral". In: *Physical Review Letters* 119.16 (2017), pp. 30–33.

[5] B.P. Abbott, LIGO Scientific Collaboration, and Virgo Collaboration. "Multi-messenger Observations of a Binary Neutron Star Merger". In: *ApJL* 848 (2017), p. L12.

[6] Jennifer Barnes and Daniel Kasen. "Effect of a high opacity on the light curves of radioactively powered transients from compact object mergers". In: *ApJ* 775.1 (2013). DOI: 10.1088/0004-637X/775/1/18.

[7] P. S. Cowperthwaite, E. Berger, and Villar, V. A., et al. "The electromagnetic counterpart of the binary neutron star merger LIGO/VIRGO GW170817. II. UV, optical, and near-ir light curves and comparison to kilonova models". In: *ApJL* 848 (2017), p. L17. ISSN: 2041-8213. DOI: 10.3847/2041-8213/aa8fc7. eprint: 1710.05840.

[8] V. A. Villar, J. Guillochon, and Berger, E., et al. "The combined ultraviolet, optical, and near-infrared light curves of the kilonova associated with the binary neutron star merger gw170817: unified data set, analytic models, and physical implications". In: *ApJL* 851.1 (2017), p. L21. ISSN: 2041-8213. DOI: 10.3847/2041-8213/aa9c84. eprint: 1710.11576. URL: http://dx.doi.org/10.3847/2041-8213/aa9c84.

[9] Kelsey A. Lund et al. "The Influence of β-decay Rates on r-process Observables". In: *The Astrophysical Journal* 944.2 (2023), p. 144. DOI: 10.3847/1538-4357/acaf56.

[10] Jonah M. Miller et al. "Full transport model of GW170817-like disk produces a blue kilonova". In: *Phys. Rev. D* 100 (2 July 2019), p. 023008. DOI: 10.1103/PhysRevD.100.023008. URL: https://link.aps.org/doi/10.1103/PhysRevD.100.023008.

[11] Kelsey Lund et al. "Magnetic Field Strength Effects on Nucleosynthesis from Neutron Star Merger Outflows". In: *The Astrophysical Journal* 964.2 (2024). DOI: 10.3847/1538-4357/ad25ef.

[12] Andreas Schröder and Daniel Schanz. "3D Lagrangian Particle Tracking in Fluid Mechanics". In: *Annual Review of Fluid Mechanics* 55 (2023). DOI: 10.1146/annurev-fluid-031822-041721.

[13] Kelsey Lund and Jonah Miller. "Neutron Star Merger Accretion Disk Trajectories for Nucleosynthesis". In: *Zenodo* (2025). DOI: 10.5281/zenodo.15352005..

[14] T. M. Sprouse and M. R. Mumpower. *PRISM, Portable Routines for Integrated nucleoSynthesis Modeling*. 2021.

[15] P. Möller et al. "Nuclear properties for astrophysical and radioactive-ion-beam applications (II)". In: *Atomic Data and Nuclear Data Tables* 125.July 2018 (2019), pp. 1–192. ISSN: 10902090. DOI: 10.1016/j.adt.2018.03.003. URL: https://doi.org/10.1016/j.adt.2018.03.003.

[16] E. M. Ney et al. "Global description of β-decay with the axially deformed Skyrme finite-amplitude method: Extension to odd-mass and odd-odd nuclei". In: *Physical Review C* 102.3 (2020), pp. 1–10. ISSN: 24699993. DOI: 10.1103/PhysRevC.102.034326.

[17] H.R. Butcher. "Thorium in G-dwarf stars as a chronometer for the Galaxy". In: *Nature* 328 (1987), pp. 127–131. DOI: 10.1038/328127a0.

[18] Anna Frebel. "From Nuclei to the Cosmos: Tracing Heavy-Element Production with the Oldest Stars". In: *Annual Review of Nuclear and Particle Science* 68.Volume 68, 2018 (2018), pp. 237–269. ISSN: 1545-4134. DOI: https://doi.org/10.1146/annurev-nucl-101917-021141. URL: https://www.annualreviews.org/content/journals/10.1146/annurev-nucl-101917-021141.